Measurement-based Characterization and Application of Low-Loss Dielectric Materials for Development of 6G Sub-THz Antennas

Ivan Ndip[#*1], Thi Huyen Le[#2], Kavin Senthil Murugesan[#3], Jens Schneider[#4], Lutz Gerhold[#5], Habib Hichri[§6], Ryohei Oishi[&7], Reki Nakano[&8], Martin Schneider-Ramelow[#†9]

[#]Fraunhofer Institute for Reliability and Microintegration, IZM, Berlin, Germany
[*]Brandenburg University of Technology Cottbus-Senftenberg (BTU), Germany
[§]Ajinomoto Fine-Techno USA Corporation, California, USA
[&]Ajinomoto Corporation Inc. Tokyo, Japan
[†]Technical University Berlin (TUB), Straße des 17. Juni 135, 10623 Berlin, Germany

ivan.ndip@izm.fraunhofer.de

Abstract

The development of high-frequency components for future 6G sub-terahertz (THz) systems is a challenging task, partly because of extremely high signal losses at sub-THz frequencies. This includes intra-system and inter-system losses. One way to overcome intra-system losses is to use packaging materials with smaller loss tangents (Df) for the development of 6G components. To overcome inter-system losses, high gain antennas and efficient power amplifiers are required to increase the equivalent isotropic radiated power (EIRP). However, these amplifiers generate heat, which may cause the values of the relative dielectric constant (Dk) and Df of the material to change with temperature. This change in Dk and Df values may degrade the performance of antennas and other components integrated in the vicinity of the amplifiers. Therefore, low-loss materials whose Dk and Df values do not fluctuate significantly with temperature are required for future 6G systems.

In this paper, we present and illustrate methods for accurate extraction of the Dk and Df values of packaging materials at sub-THz frequencies, considering a low-loss Ajinomoto Build-up Film® (ABF) material as an example. The Dk and Df values of the non-metallized and metallized ABF material were extracted in the 140 GHz band using the Fabry-Pérot and planar resonator methods, respectively. Furthermore, temperature-dependent Dk and Df values of the ABF material were also extracted up to 100°C. Our results reveal that the Dk and Df values of this material are stable over a wide range of temperatures. Finally, we used the characterized low-loss ABF material to develop a 6G sub-THz antenna array. The 1x5 elements series-fed U-slot patch antenna array was designed, fabricated and measured in the 140 GHz band. A large impedance bandwidth and high peak gain of approximately 15 GHz and 12 dBi respectively, were measured. Excellent correlation was obtained between measurement and simulation results.

Key words

6G, antenna, packaging material, dielectric constant, loss tangent, ABF

I. Introduction

6G will be the first generation of mobile communication to incorporate sensing as one of its building blocks, thus making joint communication and sensing (JCAS) an integral part of future telecommunication networks. Unlike previous generations of mobile communication, which focused on human-centric communication, 6G is expected to significantly improve autonomous machine-to-machine communication and sensing, human-to-machine communication as well as human-to-human communication. This will transform all aspects of our lives and society. To enable such transformation, 6G will also use sub-terahertz (THz) bands (between 100 GHz and 300 GHz), in addition to using sub 6 GHz and millimeter-wave (mmWave) bands. The enormous bandwidth available at sub-THz bands enables very high-resolution sensing, extremely high connection density (10^7 devices per km^2) and high channel capacity with peak data rates expected to reach up to approximately one terabit per second (1Tb/s).

However, the development of 6G systems is very challenging, partly because of extremely high signal losses at sub-THz frequencies [1]. This includes intra-system losses, caused by packaging materials and interconnects as well as inter-system atmospheric losses and signal blockage due to obstacles such as houses. To overcome intra-system losses packaging materials with smaller loss tangents (Df) are required. To overcome inter-system losses high gain antennas and numerous power amplifiers are required to increase the equivalent isotropic radiated power (EIRP). These amplifiers generate heat, which may cause the values of the relative dielectric constant (Dk) and Df to change with temperature. This change in Dk and Df values may deteriorate the performance of antennas and other components integrated in close proximity to the amplifiers. Therefore, low-loss materials whose Dk and Df values do not fluctuate significantly with temperature are required for future 6G systems. It is also of prime importance to rigorously characterize these materials with respect to frequency and temperature, and to demonstrate their suitability for 6G applications.

In some published works, the Dk and Df values of packaging materials have been extracted in the D-band for 6G [2]. To the best of the authors' knowledge, there is no single publication, in which the Dk and Df values of packaging materials have been extracted in the sub-THz bands in dependency of both temperature and frequency, and then used for the development of 6G components.

In this work, we present extensive measurement-based characterization and extraction of Dk (ε_r) and Df ($\tan\delta$) values of a low-loss dielectric material in dependency on both temperature and frequency in the 140 GHz band, and then apply the characterized material for the design and development of wide-band 6G antennas.

The thin-film dielectric material considered in this work is Ajinomoto Build-up Film® (ABF). We first applied the Fabry-Pérot method to measure 60 µm thick non-metalized ABF materials at 140 GHz. To characterize the metallized ABF, we designed microstrip-based fork-coupled resonators and measured them to extract the Dk and Df values in dependency on frequency and temperature. The characterized ABF material was used for the development of 6G antennas in the 140 GHz band. Since thin-film substrates lead to very narrow-band antennas, we applied a multi-resonance method to develop wide band 6G antennas. The designed antennas were fabricated and measured. Excellent correlation was obtained between measurement and simulation.

The remaining sections of this work are structured as follows: In section II, the Dk and Df values of non-metallized and metallized ABF material are measured and extracted in the 140 GHz band. The metallized material is also characterized to assess its dependency on temperature. The ABF material is then used for the development of 6G antennas in section III.

II. Extraction of Dk and Df Values of Non-Metallized and Metallized ABF Material for 6G

In this section, methods for extracting the Dk and Df values of non-metallized and metallized dielectrics in dependency on frequency and temperature for 6G are presented and illustrated. The Fabry-Pérot method is applied in sub-section A to extract the dielectric properties only in dependency on frequency while the planar resonator method is used in sub-section B to extract the dielectric properties in dependency on both temperature and frequency. ABF material is used as an example to illustrate the methods.

A. Extraction of Dk and Df Values of Non-Metallized Dielectrics Using Fabry-Pérot Resonator

To extract the Dk and Df values of non-metallized ABF materials, we used the Fabry-Pérot resonator method. The measurement set-up for implementing this method is shown in Figure 1. It consists of two parallel partially reflecting mirrors without any side-walls along with transmitting and receiving antennas [3]. The transmitting antenna is placed at the center of the upper reflecting mirror and the receiving antenna is placed slightly off-center in the same reflecting mirror. The functionality of these resonators is based on standing waves generated in the resonating area between the reflecting mirrors. The use of concave reflecting surfaces helps in focusing the standing waves into a smaller volume and concentrated at the center line between the two reflecting mirrors. Concave reflecting surfaces on one or both mirrors sides assist in tackling the two main limitations of the open-resonator method, such as diffraction losses at the edges and the need for precise alignment. A mode filtering aperture is positioned between the sample to be measured and the reflecting mirror to filter out additional modes in case of two or more modes. The dielectric properties of the inserted sample are calculated using the perturbation method.

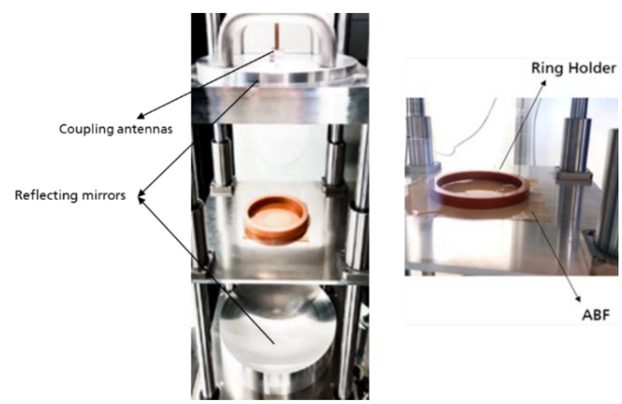

Figure 1: Measurement setup for extracting the Dk and Df values of materials using the Fabry Pérot resonator, manufactured by Keycom.

To extract the Dk and Df values, we placed a fully cured ABF film without any metallization in the Fabry-Pérot system as shown in Figure 1. The diameter of the partially reflecting mirrors is 200 mm and initial distance of separation between the mirrors is 370 mm. The resonant modes are generated between every 2-3 GHz. The resonance mode providing the highest electric field intensity will be at the center distance between the two reflecting mirrors. The cured ABF material we placed in the resonator has an area of 12x12 cm^2 and a uniform thickness of 60 µm with maximum expected deviations of ±1.5 µm. A ring holder with a diameter larger than the resonating diameter is used on the top of the sample. For the calibration of the resonator, we used a PTFE substrate as a reference material. Our measurements of the non-metallized ABF material yielded approximately 3.2 and 0.0036 respectively as ε_r and tan δ at 140 GHz [2].

B. Extraction of Dk and Df Values of Metallized Dielectrics Using Planar Resonators

In order to extract the dielectric properties of ABF material after curing, lamination, metallization and etching processes, planar microstrip fork resonator structures were designed on a 60 µm thick ABF material. An example of a 3D-model of the fork resonator structure, used for the design, is shown in figure 2. As can be seen in this figure, the fork resonator uses a capacitively coupled transmission line whose resonant frequency can be altered by changing the length. The relationship between frequency dependent permittivity, $\varepsilon_r(f)$, resonant frequency, f_r, and length, l_{eff}, of a n^{th} order resonator is given in equation (1) [4].

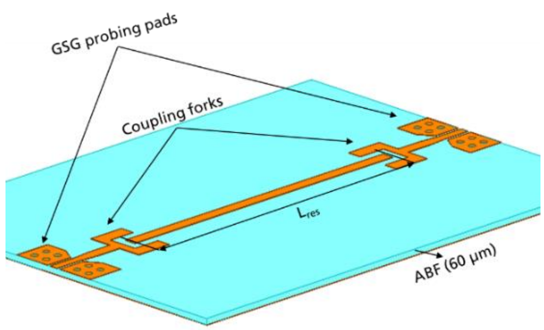

Figure 2: 3D model of a microstrip fork-coupled resonator.

$$f_r = \frac{n*c}{2*l_{eff}*\sqrt{\varepsilon_r(f)}} \qquad (1)$$

The 3D model of the planar resonator structure, shown in figure 2, was modelled and simulated using Ansys HFSS. We used the 3rd order resonance mode to extract the dielectric material properties in D-band at 122 GHz and 140 GHz, because this mode enables higher coupling between the forks and the resonating line. It also reduces the coupling between probes used for measurements. Based on the simulation results, we developed a layout of the fork resonator structure. Using the layout, test structures of the planar resonators were fabricated at Fraunhofer IZM.

Figure 3 shows the top and cross-sectional views of an examples of a fabricated resonator. After fabrication, the dimensions of geometrical parameters of the fabricated resonators were measured. Table 1 shows a comparison of these measured values and the values of the parameters used in the simulation. As can be seen in this table the deviation between these values is very small. This indicates high accuracy of the fabrication process, with very small tolerances. The roughness of the outer copper surface of the fabricated test structures was measured using a Hommel profilometer. Figure 3 (bottom) shows the measured surface roughness profile and the root mean square value of the profile, which is approximately 0.2 µm.

S-parameter measurements of the fabricated resonator structures were performed using a network analyzer from Keysight. The measurement set-up is shown in figure 4. The test structures were placed on a thermal chuck and heated up using the thermal control unit, so as to capture the impact of different temperatures on the dielectric parameters of the ABF material. The measured S-parameters were compared with the S-parameters obtained from the simulation. Figure 5 shows the excellent correlation that was obtained between measurement and simulation results. Based on this comparison, the Dk and Df values of the ABF material were extracted. To account for the impact of the surface roughness, Groisse model of finite conductivity was applied in the simulation for the surface roughness during the extraction of the Dk and Df values. The extracted values are given in table 2.

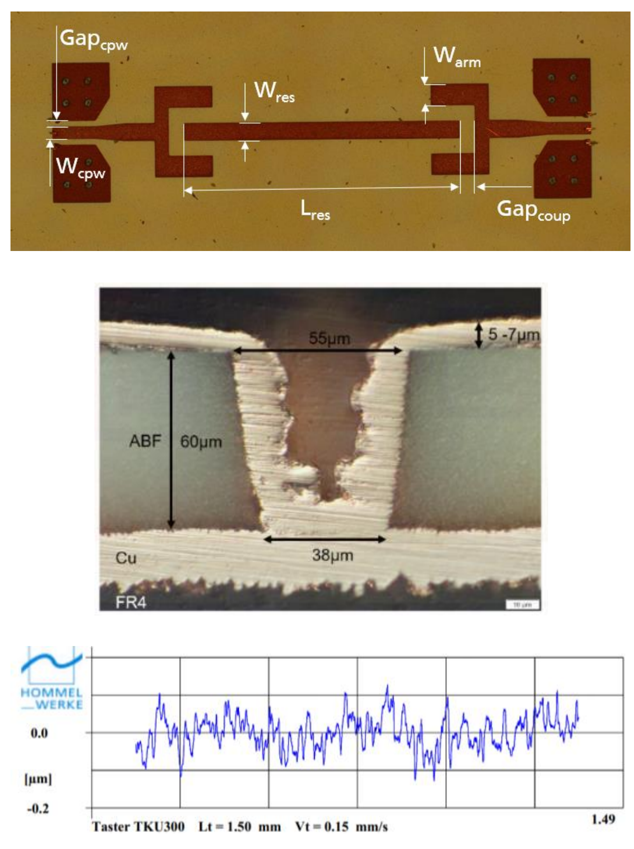

Figure 3: Microscopic image of the top view of a fabricated resonator (top); Cross-sectional view of the fabricated resonator (middle); Measured surface roughness profile of the fabricated resonator (bottom).

Table 1: Comparison between simulated and measured geometries of the 140 GHz fabricated fork resonator (see figure 3, top).

Parameter	Simulated / µm	Measured / µm
L_{res}	1900	1902
W_{res}	125	123.7
W_{arm}	150	147. 19
Gap_{coup}	100	104.31
W_{cpw}	90	87.83
G_{cpw}	35	36.91

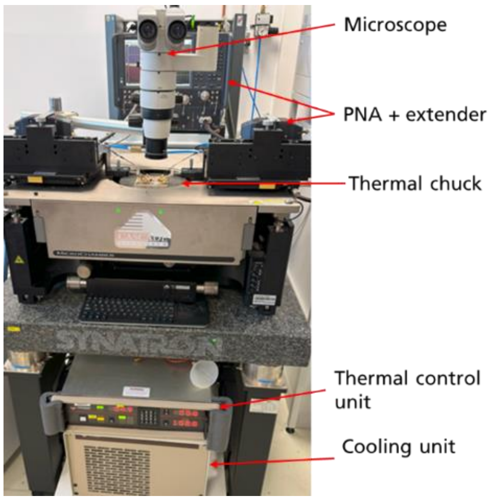

Figure 4: Measurement set-up for S-parameter measurements.

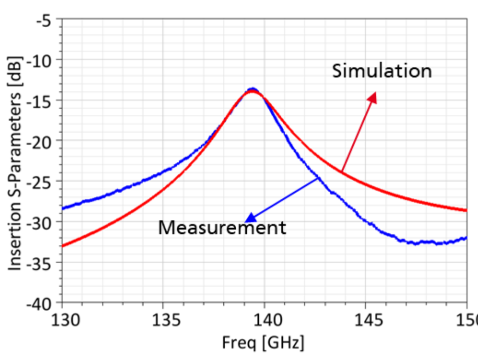

Figure 5: Simulated and measured S-parameters at 140 GHz.

Table 2: Extracted Dk and Df values of the metallized ABF material using microstrip fork coupled resonators.

Frequency	122 GHz	140 GHz
ε_r	3.33	3.315
$\tan\delta$	0.0047	0.0055

As can be seen in table 2, the extracted Dk values of the ABF material do not show significant change over a large frequency range. When compared to the non-metallized ABF material, the Df value of the metallized ABF is higher. Furthermore, it also increases with frequency. This is mainly due to several factors involved in separating the metallization losses from dielectric losses when using planar resonators, amongst which includes the following:

- Approximations in surface roughness calculations based on the measurement on the top surface of copper while the current distribution is at its highest in the bottom surface of the metallization.
- Saturation of losses due to the surface roughness at high frequencies in Groisse model applied in simulation.
- Edge effects and radiation losses present in the metallized structures at higher frequencies.

To extract the Dk and Df values based on their dependency on temperature, the thermal chuck on which the fabricated samples were placed was heated from room temperature to 100°C. To correlate the simulated and measured S-parameters at higher temperatures, different values of the copper conductivity were used in the simulation. The resistivity of copper at different temperatures is derived from the following equation:

$$R_T = R_{ref}\left(1 + \alpha\left(T - T_{ref}\right)\right) \qquad (2)$$

where R_T is the resistivity of copper at a specified temperature T and R_{ref} is the resistivity of copper at the reference temperature T_{ref}. R_{ref} at 20 °C is 1.724 x 10^{-8} (Ωm) and α is the temperature coefficient of copper and is equal to 0.00393. Conductivities of copper of 51.9 $\mathrm{M}S/m$ and 44.1 $\mathrm{M}S/m$ were incorporated into the resonator simulation of 50 °C and 100 °C respectively. The simulated and measured S-parameters of the 140 GHz resonators at 50 °C and 100 °C are shown in figure 6.

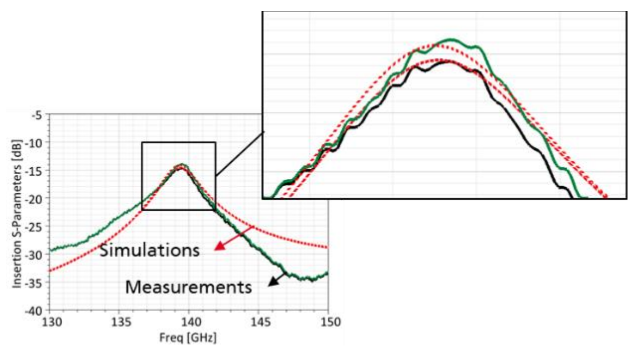

Figure 6: Simulated and measured S-parameters at 50 °C (green) and 100 °C (black) at 140 GHz.

Table 3: Extracted material properties of the ABF material using metallized fork coupled resonators at different temperatures.

Temperature	140 GHz	
	ε_r	$\tan\delta$
Room temperature	3.315	0.0055
50 °C	3.312	0.0057
100 °C	3.31	0.0065

Table 3 summarizes the extracted temperature dependent Dk and Df values. These values reveal that the dielectric properties of the characterized ABF material are stable over a wide range of temperatures up to 100 °C. This stability, coupled with the low-loss characteristics of the ABF material makes it suitable for the development of 6G systems.

III. 6G Sub-THz Antenna Array

In this section, the modeling, simulation, fabrication and measurement of a 6G sub-THz antenna array is presented.

A. Modeling and Simulation of an ABF-based 6G Antenna Array

Using the ABF material measured and characterized in the previous section, a 1x5 element series-fed 6G antenna array was modelled and simulated using Ansys HFSS. Figure 7 shows top and 3D models of the antenna that was used in the simulations. Each element in the array is a U-slot patch, and the elements are spaced by a distance of $\lambda/2$ (1.07 mm) to each other.

To improve the side lobe level behavior of the array, the Tschebyscheff-filtering method was applied to the individual elements of the array. This method is realized by using different antenna widths, which decrease with the distance from the center of the array to generate the amplitude tapering. As a result, the center patch of the array gets the most injected power and lower power is received by the outer patches, so that the side-lobes are minimized. For this purpose, the required widths of the individual patches are calculated based on the formulas in [5] for achieving a side-lobe level of about 15 dB. After applying the calculated values in the simulation, the antenna array is optimized for better impedance matching. In table 4, the simulated dimensions of the optimized 1x5 elements series-fed U-slot patch antenna array are given.

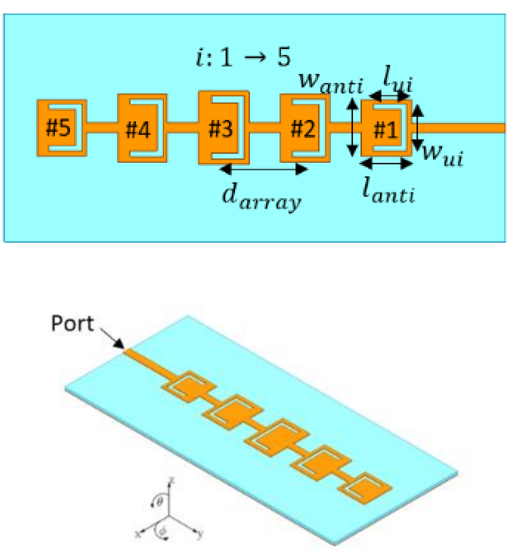

Figure 7: 3D models of a 1x5 elements series-fed U-slot patch antenna array.

Figure 8 shows the simulated return loss of the proposed 1x5 elements series-fed U-slot patch antenna array. An impedance bandwidth of about 10 GHz is achieved. The radiation patterns in E- and H-plane of the array are plotted in figure 9. The simulated array achieves a peak gain of about 12.7 dBi with a side-lobe level of 15.4 dB as calculated and a radiation efficiency of 82%.

Table 4: Simulated dimensions of the proposed 1x5 elements series-fed U-slot patch antenna array.

Parameter	**Simulated dimensions /µm**
$l_{ant1\rightarrow5}$	675
$l_{u1\rightarrow5}$	430
W_{ant1} X W_{u1}	688.5 x 555
W_{ant2} X W_{u2}	850 x 695
W_{ant3} X W_{u3}	955 x 800
W_{ant4} X W_{u4}	850 x 695
W_{ant5} X W_{u5}	688.5 x 555
W_s	80
d_{array}	1070

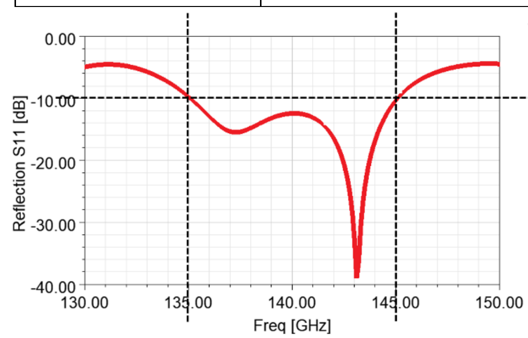

Figure 8: Simulated return loss of the proposed 1x5 elements series-fed U-slot patch antenna array.

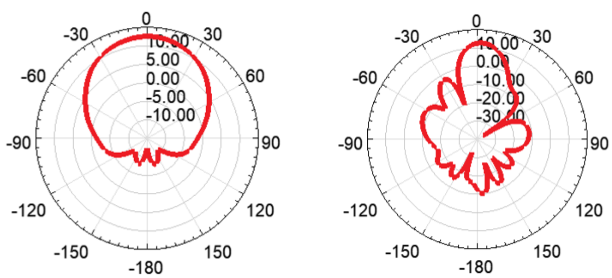

Figure 9: Radiation patterns of the proposed 1x5 elements series-fed U-slot patch antenna array: H-plane (left), E-plane (right).

B. Fabrication and Measurement of ABF-based 6G Antenna Array

Based on the simulation results, a layout of the antenna array was developed and used for the fabrication. The test structures of the antenna array were fabricated on a 60 µm ABF material at Fraunhofer IZM. To improve the mechanical stability of the test structures, a standard FR4 core fully coated with copper was used as a support during the fabrication. Afterwards, the ABF was laminated onto this carrier. For the GSG probing section, blind vias (BV) with an aspect ratio 1:1, i.e. drill hole of 60 µm diameter, were laser drilled to contact the ground probing pads to the reference plane of the antenna. Finally, the top layer was structured by seed layer sputtering and plating. The metal thickness of the top layer reached approximately 5-7 µm. Figure 10 shows the top view of the fabricated antenna array test structure. In order to characterize the antenna performance, probing pads for RF probes in GSG configuration was added to the simulated antennas.

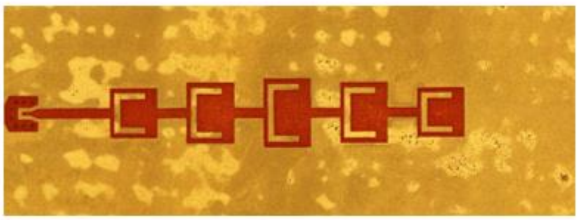

Figure 10: Fabricated 1x5 elements series-fed U-slot patch antenna test structure.

Table 5: Comparison between simulated and measured dimensions of the proposed 1x5 elements series-fed U-slot patch antenna array.

Parameter	Simulated/µm	Measured/µm
$l_{ant1\rightarrow5}$	675	673
$l_{u1\rightarrow5}$	430	439
w_{ant1} x w_{u1}	688.5 x 555	694 x 564
w_{ant2} x w_{u2}	850 x 695	850 x 707
w_{ant3} x w_{u3}	955 x 800	965 x 808
w_{ant4} x w_{u4}	850 x 695	851 x 707
w_{ant5} x w_{u5}	688.5 x 555	692 x 564
w_s	80	81.32
d_{array}	1070	1080

A comparison of the geometries of the fabricated and designed antenna configurations is given in table 5. The measured dimensions of the fabricated test samples show a maximum fabrication tolerance of approximately 2.1% compared to the original design. Using the measured dimensions, the simulation model of the antenna array was adapted.

The return loss of the fabricated antenna array was measured using a network analyzer from Keysight, which is connected to Frequency Extender Modules in the frequency range between 125 GHz to 145 GHz. In figure 11, the measured and simulated return losses are compared. As can be seen in figure 11, a very good correlation was obtained between measurement and simulation results. A measured impedance bandwidth of about 15.2 GHz is achieved compared to the simulated value of 14 GHz. In figure 12 the comparison between simulated and measured radiation patterns in the E- and H-planes is shown. A measured peak gain of the array is about 12 dBi, whereas the simulated gain is 12.2 dBi. Excellent correlation was also obtained between the measured and simulated radiation patterns.

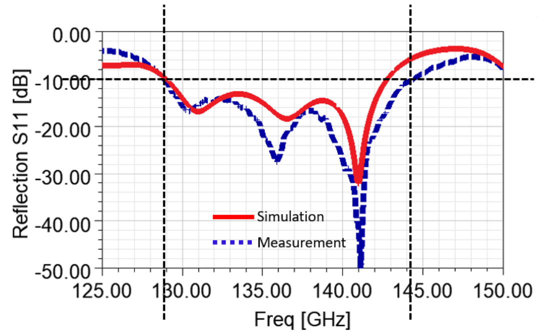

Figure 11: Comparison between the simulated and measured return losses of the proposed 1x5 elements series-fed U-slot patch antenna array.

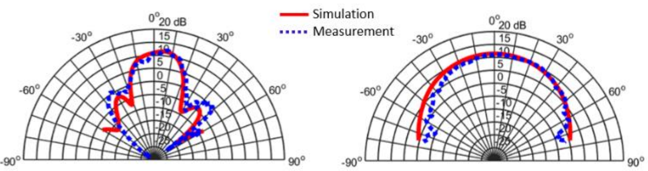

Figure 12: Comparison between the simulated and measured radiation patterns of the proposed 1x5 elements series-fed U-slot patch antenna array: E-plane (left), H-plane (right).

III. Conclusion

We present two methods for extracting the Dk and Df values of packaging materials at sub-THz frequencies for 6G applications. To illustrate these methods, we used an ABF material as an example. The Dk and Df values of non-metallized and metallized low-loss ABF material were extracted in the 140 GHz band using the Fabry-Pérot and planar resonator methods, respectively. Stable values of Dk and Df of the material were also observed over a wide range of frequencies up to 100°C. This stability, coupled with the low-loss characteristics of the ABF material makes it suitable for the development of 6G components. Finally, we used the characterized ABF material to develop a 6G sub-THz antenna array. Excellent correlation was obtained between measurement and simulation results.

References

[1] T. H. Le et al., "Wideband Antennas on Thin-Film Packaging Substrates for 140 GHz 6G Applications," *2024 IEEE 74th Electronic Components and Technology Conference (ECTC)*, Denver, CO, USA, 2024, pp. 732-737

[2] K. S. Murugesan et al., "Temperature dependent Dielectric Characterization of Low Loss Thin Film Polymer up to sub-THz bands," *2024 IEEE 74th Electronic Components and Technology Conference (ECTC)*, Denver, CO, USA, 2024, pp. 865-870

[3] Clarke, R. N., and C. B. Rosenberg. "Fabry-Perot and open resonators at microwave and millimetre wave frequencies, 2-300 GHz." *Journal of Physics E: Scientific Instruments*, Volume 15, Issue 1, pp. 9-24 (1982).

[4] A. H. Muqaibel, A. Safaai-Jazi and S. M. Riad, "Fork-Coupled Resonators for High-Frequency Characterization of Dielectric Substrate Materials," in *IEEE Transactions on Instrumentation and Measurement*, vol. 55, no. 6, pp. 2216-2220, Dec. 2006

[5] Constantine A. Balanis, Antenna Theory Analysis and Design, 3rd ed., Hoboken, New Jersey, 2005, pp.331-337